



Genetic lesions in *MYC* and *STAT3* drive oncogenic transcription factor overexpression in plasmablastic lymphoma

Julia Garcia-Reyero,^{1,2} Nerea Martinez Magunacelaya,² Sonia Gonzalez de Villambrosia,³ Sanam Loghavi,⁴ Angela Gomez Mediavilla,² Raul Tonda,⁵ Sergi Beltran,⁵ Marta Gut,⁵ Ainara Pereña Gonzalez,² Emmanuel D'Àmore,⁶ Carlo Visco,⁷ Joseph D. Khoury⁴ and Santiago Montes-Moreno^{1,2}

¹Anatomic Pathology Service, Hospital Universitario Marqués de Valdecilla/IDIVAL, Universidad de Cantabria, Santander, Spain; ²Translational Hematopathology Laboratory, IDIVAL, Centro de Investigación Biomédica en Red de Cáncer (CIBERONC), Santander, Spain; ³Cytogenetics Unit, Department of Hematology, HUMV, Santander, Spain; ⁴Hematopathology Department, MD Anderson Cancer Center, Houston, TX, USA; ⁵Centre Nacional d'Anàlisi Genòmica. Barcelona Institute of Science and Technology (BIST). Universitat Pompeu Fabra, Barcelona, Spain; ⁶Departments of Pathology and Hematology, San Bortolo Hospital, Vicenza, Italy and ⁷Department of Medicine, Section of Hematology, University of Verona, Verona, Italy

Haematologica 2021
Volume 106(4):1120-1128

ABSTRACT

The mutational profile of plasmablastic lymphoma has not been described. We performed a targeted, exonic next-generation sequencing analysis of 30 plasmablastic lymphoma cases with a B-cell lymphoma-dedicated panel and fluorescence *in situ* hybridization for the detection of *MYC* rearrangements. Complete phenotyping of the neoplastic and microenvironmental cell populations was also performed. We identified an enrichment in recurrent genetic events in *MYC* (69% with *MYC* translocation or amplification and three cases with missense point mutations), *PRDM1*/Blimp1 and *STAT3* mutations. These gene mutations were more frequent in Epstein-Barr virus (EBV)-positive disease. Other genetic events included mutations in *BRAF*, *EP300*, *BCR* (*CD79A* and *CD79B*), *NOTCH* pathway (*NOTCH2*, *NOTCH1* and *SGK1*) and *MYD88* pL265P. Immunohistochemical analysis showed consistent *MYC* expression, which was higher in cases with *MYC* rearrangements, together with phospho-*STAT3* (Tyr705) overexpression in cases with *STAT3* SH2 domain mutations. Microenvironmental cell populations were heterogeneous and unrelated to EBV, with enrichment of tumor-associated macrophages (TAM) and PD1-positive T cells. PD-L1 was expressed in all cases in the TAM population but only in the neoplastic cells in five cases (4 of 14 EBV-positive cases). HLA expression was absent in the majority of cases of plasmablastic lymphoma. In summary, the mutational profile of plasmablastic lymphoma is heterogeneous and related to EBV infection. Genetic events in *MYC*, *STAT3* and *PRDM1*/Blimp1 are more frequent in EBV-positive disease. An enrichment in TAM and PD1 reactive T lymphocytes is found in the microenvironment of plasmablastic lymphoma and a fraction of the neoplastic cells express PD-L1.

Correspondence:

SANTIAGO MONTES MORENO
santiago.montes@scsalud.es

Received: March 1, 2020.

Accepted: April 9, 2020.

Pre-published: April 9, 2020.

<https://doi.org/10.3324/haematol.2020.251579>

©2021 Ferrata Storti Foundation

Material published in *Haematologica* is covered by copyright. All rights are reserved to the Ferrata Storti Foundation. Use of published material is allowed under the following terms and conditions:

<https://creativecommons.org/licenses/by-nc/4.0/legalcode>.

Copies of published material are allowed for personal or internal use. Sharing published material for non-commercial purposes is subject to the following conditions:

<https://creativecommons.org/licenses/by-nc/4.0/legalcode>,

sect. 3. Reproducing and sharing published material for commercial purposes is not allowed without permission in writing from the publisher.



Introduction

Plasmablastic lymphoma (PBL) is an aggressive type of non-Hodgkin B-cell lymphoma defined as a high-grade large B-cell neoplasm with plasma cell phenotype (i.e., loss of B-cell antigens with downregulation of CD20 and PAX5 expression and overexpression of PRDM1/Blimp1 and XBP1s).¹⁻⁴

Epstein-Barr virus (EBV) infection is found in the majority of cases but is not required for the development of a plasmablastic phenotype since clear-cut PBL can be negative for EBV.^{3,5} In addition, recent evidence suggests that EBV or human immunodeficiency virus (HIV) status does not influence the gene expression profile

patterns of PBL.⁶ However EBV positivity in PBL has been found to be associated with increased expression of the programmed death ligand 1 (PD-L1) protein as well as other immune escape markers,^{7,8} and decreased expression of major histocompatibility class II (MHCII)/human leukocyte A (HLA)-DR molecules by the neoplastic cells.⁹ This has recently been found to be associated with increased antiviral cytotoxic immunity involving different immune cell populations.⁷

The genetic landscape of somatic mutations in PBL is unclear. So far, *MYC-IGH* translocations have been the most commonly detected alterations, being present in 60% of cases.^{10,11} Concurrent mutations in *PRDM1/Blimp1* have been found in half of these cases.¹² Very recently, exome sequencing of a series of HIV-positive cases of PBL showed somatic mutations involving components of the non-canonical NF κ B pathway as well as genes involved in immune response,¹⁵ but the data remain limited.

Our aim was to characterize the genetic profile of a series of PBL cases using targeted exonic next-generation sequencing (NGS) and correlate the findings with EBV infection and the expression status of immune checkpoint proteins in both the population of neoplastic cells and cells in the microenvironment. In addition, we quantified the components of the microenvironment and searched for skewed T-cell populations in this tumor. We found that the mutational profile of PBL was related to EBV infection in the tumor cells and identified recurrent genetic events in *MYC*, *STAT3* and *PRDM1/Blimp1* that were more frequent in EBV-positive disease. In addition, we identified PD-L1 expression on tumor cells in a subset of cases as well as enrichment of tumor-associated macrophages (TAM) and programmed death 1 (PD1) reactive T cells in the microenvironment of PBL cases.

Methods

Case selection

Twenty-eight new cases were retrieved from the files of the Pathology Department of Universitario Marqués de Valdecilla Hospital (Santander, Spain), ten samples from the files of the University of Texas MD Anderson Cancer Center Hematopathology Department (Houston, TX, USA) and four cases from the Pathology Department of San Bortolo Hospital (Vicenza, Italy). Material transfer agreements were signed by the Instituto de Investigación Marqués de Valdecilla (IDIVAL) and corresponding institutions to share the material in the project. The study and sample collection were approved by the local ethics committee (CEIC Cantabria, Institutional Review Board code 2016.168) and complied with the Declaration of Helsinki. All cases were diagnosed according to the World Health Organization (WHO) classification of Hematolymphoid Neoplasms.¹⁴ All cases had to be negative for pan-B-cell markers (CD20), HHV-8 and ALK in order to be included in the study. The phenotype of the cases was consistent with a plasma cell differentiation program.^{4,15} The clinical features of the cases were recorded and a summary is available in *Online Supplementary Table S1*.

Immunohistochemistry and *in situ* hybridization

Immunohistochemical reactions were performed following conventional automated procedures. Chromogenic *in situ* hybridization for EBV and its encoding RNA (EBER)

and fluorescence *in situ* hybridization (FISH) for the detection of *MYC* rearrangements were also done.

Quantification of the cellular composition of the tumor and transcription factor abundance

The different lymphoid and histiocytic/dendritic subpopulations, identified with CD3, CD8, PD1, CD163, PD-L1 and MHCII/HLA DP/DR and the absolute number of nuclei showing expression of *MYC* and phospho-STAT3 (Tyr705) were quantified.

Next-generation sequencing using amplicon-based library generation

DNA was extracted from formalin-fixed paraffin-embedded samples using the PicoPure™ DNA Isolation Kit (ThermoFisher Scientific) and was quantified by an Qbit fluorometer (ThermoFisher Scientific). All samples subjected to NGS analysis were required to have >50% of neoplastic cells, identified by morphology (hematoxylin & eosin).

A TruSeq® Custom Amplicon Low Input Library containing exonic regions of 35 selected genes of interest was used to isolate the DNA for sequencing (Illumina). The selected genes were *CARD11*, *ARID1A*, *NOTCH1*, *TCF3*, *SMARCA4*, *STAT6*, *EP300*, *CREBBP*, *MLL2*, *BTK*, *NOTCH2*, *TNFRSF14*, *ATM*, *FOXO1*, *B2M*, *PLCG2*, *CD79B*, *TP53*, *STAT3*, *BCL2*, *MEF2B*, *CD79A*, *CXCR4*, *PTPN1*, *MYD88*, *FAT2*, *PRDM1*, *TNFAIP3*, *SGK1*, *CCND3*, *PIM1*, *EZH2*, *BRAF*, *MYC* and *NOTHC2*. Of note, variants occurring in regions outside the coverage of our targeted design were not explored using this approach. Details about library preparation can be found in the *Online Supplementary Material*.

Sequencing was performed using a HiSeq instrument (Illumina, paired end, 2x150) at the National Genomic Analysis Center (CNAG, Barcelona, Spain).

Sequencing data interpretation and reporting

Only variants in which both libraries had a coverage ≥ 300 reads and had the same genotype were selected for downstream analysis. Subsequently only missense, frameshift, and nonsense somatic mutations with a variant frequency >10% were considered (*Online Supplementary Table S2*). Single nucleotide polymorphisms were filtered out using variant allele frequency criteria, and with comparison with dbSNP and an in-house database of germline variants. Finally, 34 somatic mutations (31 missense, 3 nonsense) in 14 genes were considered (Table 1).

Further details on the methods are provided in the *Online Supplementary Material*.

Results

The mutational profile of plasmablastic lymphoma is heterogeneous and correlates with Epstein-Barr virus infection in the neoplastic cells

After targeted NGS with a lymphoma-dedicated panel, somatic missense and nonsense mutations were identified in 18 out of 30 PBL cases (60%). EBV-negative cases tended to show a higher rate of mutations, as compared to EBV-positive cases (87.5% vs. 54%, respectively; χ^2 test, $P > 0.05$) (Figure 1).

Interestingly the pattern of mutations was also different

Table 1. Summary of the mutations found in 18 out 30 cases (60%) of plasmablastic lymphoma analyzed by targeted exonic next-generation sequencing.

ID	Gene	Location chromosome	Domain	Allele	cDNA position	Codons	AA change	Consequence*	Existing_variation	
4	<i>STAT3</i>	17	---	A	2009	Gac/Tac	566	D/Y	deleterious	COSM220689
4	<i>EP300</i>	22	---	A	7249	atG/atA	2010	M/I	tolerated	---
11	<i>MYC</i>	8	---	G	578	aCc/aGc	23	T/S	tolerated	---
11	<i>MYC</i>	8	---	A	775	Tac/Aac	89	Y/N	tolerated	---
11	<i>MYC</i>	8	---	C	899	tTc/tCc	130	F/S	deleterious	COSM4171775
11	<i>MYC</i>	8	---	G	945	atC/atG	145	I/M	deleterious	---
14	<i>STAT3</i>	17	SH2	A	2255	Atg/Ttg	648	M/L	tolerated	---
14	<i>STAT3</i>	17	SH2	A	2232	tAc/tTc	640	Y/F	probably damaging	COSM1155743
17	<i>STAT3</i>	17	SH2	G	2165	Ggc/Cgc	618	G/R	deleterious	COSM1166777
17	<i>PRDM1</i>	6	PR	G	843	gaC/gaG	203	D/E	neutral	rs811925*, COSM4160094
28	<i>PRDM1</i>	6	PR	G	843	gaC/gaG	203	D/E	neutral	rs811925*, COSM4160094
7	<i>MYC</i>	8	---	T	1085	tAc/tTc	192	Y/F	probably damaging	---
7	<i>CD79B</i>	17	---	T	175	Gac/Aac	34	D/N	tolerated	---
8	<i>SMARCA4</i>	19	---	A	3295	cGa/cAa	1005	R/Q	deleterious	---
8	<i>PRDM1</i>	6	Ac	A	2546	gGc/gAc	771	G/D	tolerated	---
2	<i>STAT3</i>	17	SH2	A	2253	aAc/aTc	647	N/I	deleterious	COSM1155744
2	<i>NOTCH1</i>	9	EGF-like	A	1278	cCc/cTc	401	P/L	deleterious	COSM4745915
5	<i>STAT3</i>	17	SH2	A	2232	tAc/tTc	640	Y/F	probably damaging	COSM1155743
10	<i>PRDM1</i>	6	Pro-rich	A	1295	aGc/aAc	354	S/N	tolerated	rs143040512, COSM4406870
10	<i>CD79A</i>	19	---	A	413	tgG/tgA	76	W/*	---	COSM5493940
26	<i>PRDM1</i>	6	PR	G	843	gaC/gaG	203	D/E	neutral	rs811925*, COSM4160094
27	<i>PRDM1</i>	6	PR	G	843	gaC/gaG	203	D/E	neutral	rs811925*, COSM4160094
3	<i>ARID1A</i>	1	---	A	762	Ggg/Agg	131	G/R	deleterious	---
3	<i>ARID1A</i>	1	---	C	6526	tGc/tCc	2052	C/S	deleterious	---
3	<i>MYD88</i>	3	TIR	C	794	cTg/cCg	265	L/P	deleterious	COSM85940
15	<i>BRAF</i>	7	ATP binding site	G	1467	gGa/gCa	469	G/A	deleterious	COSM460
18	<i>SGK1</i>	6	---	A	1950	tCc/tTc	451	S/F	deleterious	---
18	<i>SGK1</i>	6	---	A	1737	gCt/gTt	380	AV	tolerated	---
9	<i>NOTCH2</i>	1	PEST	A	7418	Cga/Tga	2400	R/*	deleterious	COSM36210
1	<i>MYC</i>	8	---	T	747	agC/agT	79	S/	---	---
1	<i>EP300</i>	22	---	A	6411	cGc/cAc	1731	R/H	deleterious	---
1	<i>BRAF</i>	7	STKc_Raf	T	1860	gTg/gAg	600	V/E	deleterious	COSM476
1	<i>SGK1</i>	6	---	A	1004	Aag/Tag	136	K/*	deleterious	---
13	<i>TP53</i>	17	---	T	1008	cGt/cAt	273	R/H	possibly damaging	COSM10660

Gene name, exonic location, cDNA position, single nucleotide change observed, and amino acid change predicted, together with consequences predicted using three different algorithms are shown. In addition, the dbSNP and the COSMIC identity is provided when available. ID: identity; AA: amino acid.

between EBV-positive and EBV-negative cases. Recurrent somatic mutations restricted to EBV-positive cases were found in *PRDM1*/Blimp1 in six cases and in *STAT3* in five cases. Notably, a recurrent *PRDM1*/Blimp1 variant, D203E, was identified in four out of six cases, involving the PR domain of the protein.

STAT3 mutations were found in five out of 30 cases (16%), all EBV-positive. Interestingly all but one (*STAT3*pD566Y) of the mutations involve the SH2 domain of *STAT3* protein (*STAT3*pY640F, *STAT3*pM648L, *STAT3*pG618R, *STAT3*pN647I) (Figure 2) and lead to phospho-*STAT3* (Tyr705) protein overexpression (see below).

The majority of PBL cases (16 out of 23 tested, 69%) harbored structural abnormalities at the *MYC* locus. Fourteen cases were found to have a *MYC* translocation (60%) using break apart probes. *MYC-IGH* was confirmed in seven of

nine cases tested (77%). *MYC* was found to be amplified by FISH in two additional cases (Figure 1). Thus, in cases with *MYC* rearrangements, *MYC-IGH* was the most frequent alteration. Although there was a clear trend for an association between EBV positivity and *MYC* rearrangement the difference was not statistically significant (χ^2 test, $P=0.06$).

Furthermore, *MYC* was found to be mutated in three cases with all but one of the mutations involving exon 2 and consisting of transversions and transitions at C: G pairs (4 out of 7 mutations) (Table 1). Furthermore, the *MYC*p79S mutation involves the WRCY consensus motif. All these features are consistent with a mechanism related with aberrant somatic hypermutation, as described in early reports.¹⁶

Mutations common mutations diffuse large B-cell lymphoma (DLBCL), not otherwise specified (NOS), involving B-cell receptor (BCR) activation, TLR/NF κ B, histone-mod-

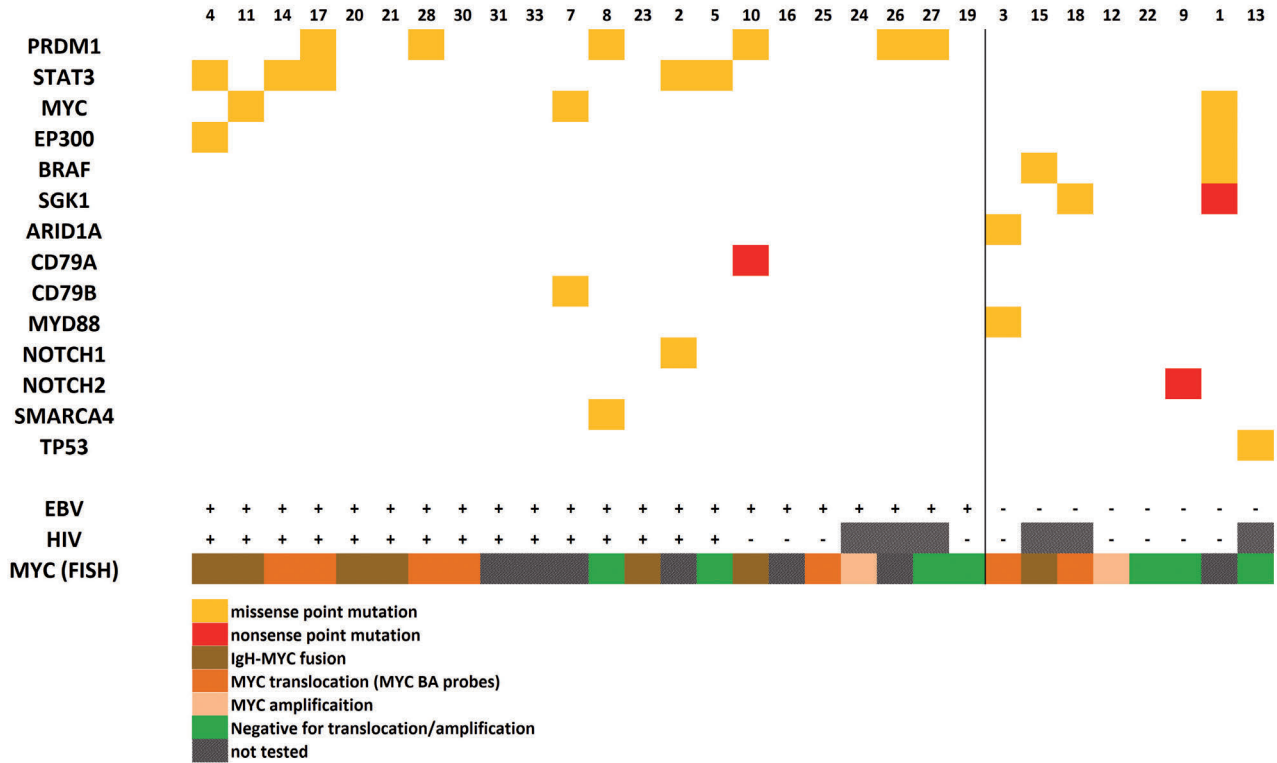


Figure 1. Summary of the mutations found in 18 out of 30 cases (60%) analyzed by targeted exonic next-generation sequencing. Epstein-Barr virus (EBV) positivity of tumor cells and human immunodeficiency virus (HIV) infection by the patient are shown, together with the status of the MYC gene as determined by interphase fluorescence *in situ* hybridization (FISH). The pattern of somatic mutations is heterogeneous with a trend to a higher rate of mutations in EBV-positive cases. The most common genetic events in plasmablastic lymphoma are mutations (including translocations, amplifications and point mutations) in the MYC gene. Previously undescribed abnormalities in plasmablastic lymphoma such as STAT3 (16% of cases), BRAF, MYD88, NOTCH2 and TP53 mutations were also identified (see details in Table 1).

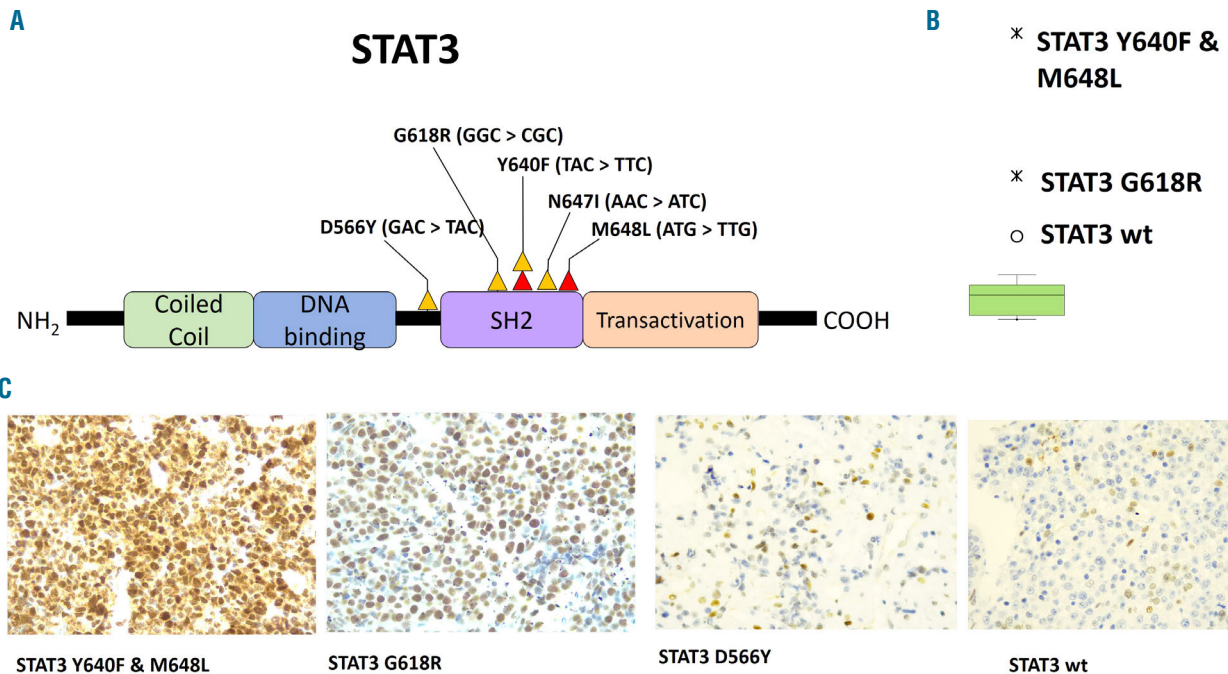


Figure 2. STAT3 mutations in plasmablastic lymphoma. (A) STAT3 mutations were found in five cases (16%), all of which were positive for Epstein-Barr virus. Interestingly all but one (STAT3pD566Y) of the mutations involved the SH2 domain of the STAT3 protein. (B) The mean phospho-STAT3 expression for SH2 domain-mutated cases (2 cases with available mutational and immunohistochemical data) was 249 nuclei per high power field (40x), whereas that for STAT3 wild-type cases was 28 nuclei per high power field. Thus, STAT3 SH2 domain mutations led to phosphoSTAT3 (Tyr705) protein overexpression. (C) Representative microphotographs of phosphoSTAT3 (Tyr705) protein expression in plasmablastic lymphoma.

ifying genes and the NOTCH pathway were found in eight cases (Table 1, Figure 1). These mutations involved *CD79pAW76**, *CD79BpD34N*, *MYD88pL265P*, *NOTCH1pP401L*, *NOTCH2pR2400**, *SGK1Kp136** and *EP300pM2010L/EP300pR1731H*. The NOTCH pathway was affected by somatic mutations in NOTCH2 (1 case), NOTCH1 (1 case) and SGK1 (2 cases). Other mutations found were *SMARCA4pR1005Q* and *TP53pR273H*. Of note, two cases, both EBV-negative, had mutations in the *BRAF* gene, one case with the canonical activating *BRAFpV600E* mutation and the other with a *BRAFpG469A* mutation in the ATP binding site.

STAT3 mutations are associated with constitutive phospho-STAT3 (Tyr705) activation and MYC protein overexpression is related to MYC rearrangement status

Expression of phospho-STAT3 (Tyr705) protein was quantified immunohistochemically in 20 cases with available mutational data. Mean phospho-STAT3 expression was 48 nuclei per high power field (HPF; 40x) in these 20 cases. Mean expression for two out of four SH2 domain-mutated cases with available immunohistochemical data was 249 nuclei per HPF. Mean phospho-STAT3 expression for *STAT3* wild-type cases was 28 nuclei per HPF. Mean phospho-STAT3 expression for the single non-SH2 *STAT3*-mutated sample was 40 nuclei per HPF. Thus, *STAT3* SH2 domain mutations (*STAT3pY640F*, *STAT3pM648L*, *STAT3pG618R*, *STAT3pN647I*) were associated with overexpression of phospho-STAT3, as determined by immunohistochemistry of tissue samples (Figure 2B).

MYC protein was consistently expressed in all the cases (range, 59-236 nuclei per HPF; mean 236), irrespective of the presence of *MYC* translocations, as previously report-

ed.^{12,17} However, significant differences in the level of *MYC* expression were found, according to *MYC* gene status. *MYC*-translocated (14 cases) and -amplified cases (2 cases) had, as expected, higher *MYC* protein expression than cases without *MYC* rearrangements (7 cases). The mean number of positive nuclei per HPF was 109 in non-rearranged cases *versus* 282 in *MYC*-rearranged cases (Mann-Whitney test, $P < 0.0001$) (Figure 3).

Mean *MYC* protein expression in 22 cases with available data was 236 nuclei per HPF, which was significantly higher than the mean 48 nuclei per HPF in the cases of phospho-STAT3 protein expression (Wilcoxon test, $P < 0.001$). There was no correlation between the levels of expression of the two proteins (Pearson test, non-significant). Due to the high prevalence of *MYC* translocations and amplification in PBL and the relatively low levels of phospho-STAT3 expression and absence of correlation between the proteins, it is unlikely that *STAT3* activation contributed to *MYC* overexpression in most cases. However, one of our cases with *STAT3* SH2 domain mutations and absence of *MYC* translocation by FISH showed high levels of both phospho-STAT3 and *MYC* proteins, without detectable *PRDM1*/*Blimp1* mutations, suggesting that *MYC* overexpression might be related with *STAT3* activation by mutations in rare cases of PBL.

In summary, *MYC* protein overexpression is due to rearrangements involving *MYC* in a significant proportion of cases of PBL (69% in our series). Most translocations fuse *MYC* to *IGH* and a few cases may show amplifications of the *MYC* gene. Both alterations lead to *MYC* protein overexpression. Genetic alterations in the *MYC* regulatory domains of *PRDM1*/*Blimp1* may also contribute to its overexpression.¹² In addition here we show that a frac-

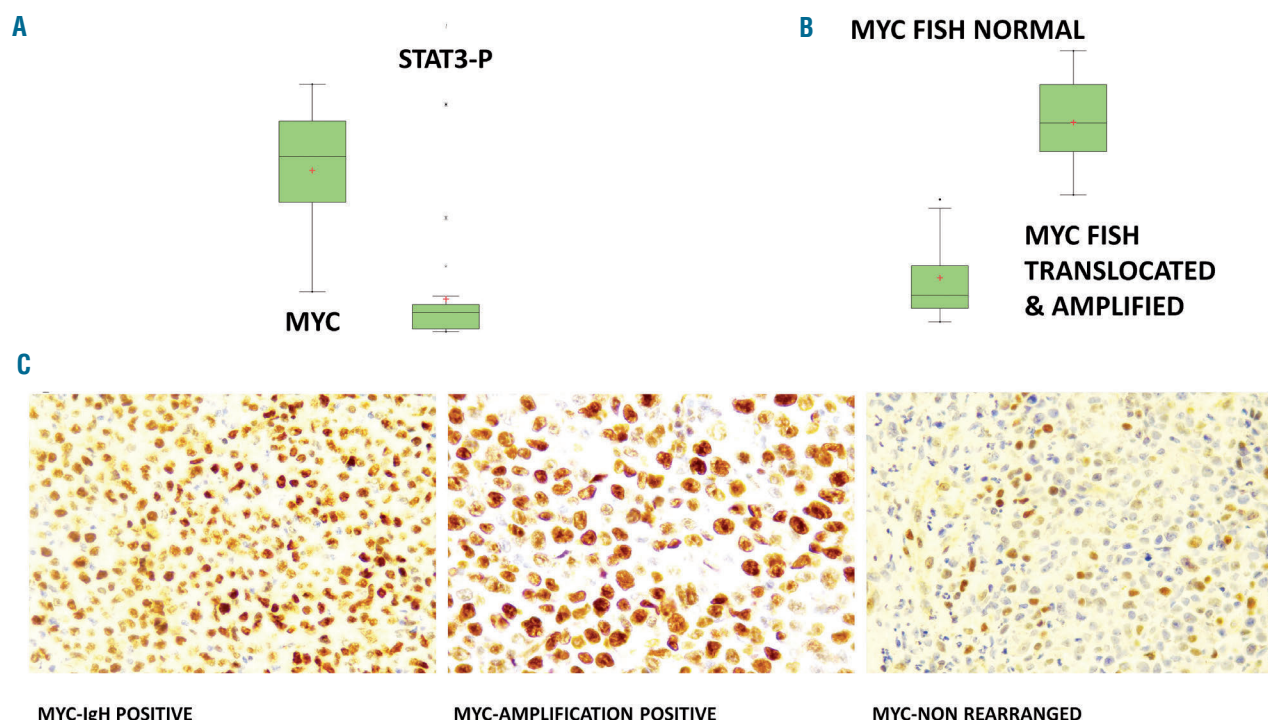


Figure 3. MYC protein expression in plasmablastic lymphoma. (A) MYC protein was consistently expressed in the cases of plasmablastic lymphoma. (A) Mean *MYC* protein expression in 22 cases with available data was 236 nuclei per high power field (HPF), which was significantly higher than the mean of 48 nuclei per HPF in the case of phospho-STAT3 protein expression (Wilcoxon test, $P < 0.001$). *MYC* translocated cases ($n=14$) and *MYC* amplified cases ($n=2$) had higher *MYC* protein expression than cases without *MYC* rearrangements ($n=7$) (Mann-Whitney test, $P < 0.0001$). (C) Representative microphotographs of *MYC* protein expression in plasmablastic lymphoma.

tion of PBL cases has STAT3 activation due to somatic mutations in the *STAT3*-SH2 domain that may increase MYC expression, as previously described in DLBCL¹⁸ (Figure 4).

Phenotype of the immune microenvironment and neoplastic cells in plasmablastic lymphoma

We quantified the expression of CD163 and PD-L1 in histiocytic/dendritic cells in the cases of PBL. The mean expression of PDL1 was 33 nuclei per HPF (range, 1.67-61) and the mean expression of CD163 was 38 nuclei per HPF (range, 2-84) (Figure 5). The correlation between CD163 and PD-L1 expression was statistically significant (Pearson 0.6, $P < 0.05$), suggesting that PD-L1-positive cells are histiocytes in PBL. There was not a significant difference in the content or distribution of CD163 and PD-L1-positive histiocytes between EBV-positive and EBV-negative cases (Mann-Whitney test, $P > 0.05$).

CD8-positive and PD1-positive T-cell subpopulations were quantified. The mean number of CD8-positive lymphocytes was 52 nuclei per HPF (range, 1-117) and the mean number of PD1-positive lymphocytes was 32 nuclei per HPF (range, 0-76). There was a significant difference in the distribution of CD8 and PD1-positive cell subsets (Wilcoxon test, $P < 0.001$) consistent with different cell populations. The Pearson correlation value was however statistically significant (Pearson 0.59, $P < 0.05$). There was no significant difference in the content and distribution of CD8 or PD1-positive lymphocytes between EBV-positive and EBV-negative cases (Mann-Whitney test, $P > 0.05$) (Figure 5).

PD-L1 was expressed by tumor cells in five out of 24 (20%) cases evaluated (mean 59 nuclei per HPF; range, 25-98). Four out of five PD-L1-positive cases (in the neoplastic cells) were EBV-positive. Fourteen EBV-positive PBL cases were negative for PD-L1 in the tumor cells. Thus four out of 18 (22%) EBV-positive PBL cases were PD-L1-positive, while one out of six (16%) EBV-negative cases was PD-L1-positive. Thus, there was no association between EBV infection by tumor cells and PD-L1 expression, since most of the EBV-positive cases were PD-L1-negative ($P = \text{non-significant}$) (Figure 5). Interestingly one case with *STAT3* SH2 mutations showed concurrent PD-L1 and phospho-STAT3 (Tyr705) expression. PD-L1 expression data were

not available for the other *STAT3* SH2-mutated cases to test this association.

Consistent with previously published data,⁹ MHCII protein/HLA (DP, DR) was virtually absent in PBL. Only three cases out of 25 tested were positive (12%, mean 349 nuclei per HPF; range, 284-440). Two cases showed a membranous and cytoplasmic granular pattern and the other a membranous pattern. All three cases were EBV-positive. The other 22 cases were completely negative for HLA expression in tumor cells (Figure 5).

Discussion

In this study we characterized the genetic profile of a series of cases of PBL using targeted exonic NGS, any correlations with EBV infection and the expression of immune checkpoint proteins in both the neoplastic population and tumor microenvironment. We found that genetic abnormalities (including translocations, amplifications and point mutations) in the *MYC* gene were the most common genetic event in PBL. In addition to previously described translocations, involving *IGH* and *MYC*,^{10,11} here we found that a few cases may have *MYC* amplification, confirming our previous observations.¹² Both *MYC* translocations and amplifications lead to a significantly increased expression of MYC protein. Interestingly we also identified *MYC* point mutations, mainly consisting of transversions and transitions at C:G pairs and involving exon 2 and, in the case of *MYC*p79S mutation, the WRCY consensus motif. All these features are consistent with a mechanism related to aberrant somatic hypermutation.¹⁶ The oncogenic effect of these point mutations does, however, remain unclear.

We also found that 16% of our cases (5 cases) carried recurrent somatic mutations in the oncogene *STAT3*, preferentially involving the SH2 domain of the protein. Interestingly these mutations were restricted to EBV-positive PBL. Here we demonstrate that these mutations led to increased expression of phospho-STAT3 (Tyr705).

STAT3 mutations and phospho-STAT3 overexpression have been found very rarely in DLBCL NOS (6% according to Ohgami *et al.*¹⁹). In cases of ALK-positive large B-cell lymphomas, which commonly show a plasmablastic phe-

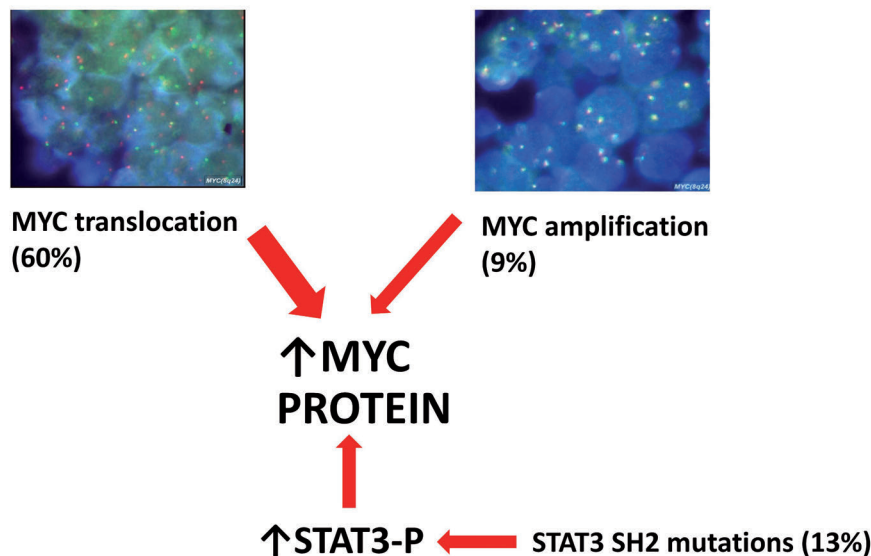


Figure 4. MYC protein overexpression in plasmablastic lymphoma. MYC protein overexpression is due to rearrangements involving *MYC* in a significant proportion of cases of plasmablastic lymphoma (69% in these series). Most translocations fuse *MYC* to *IGH* and a few cases may show amplifications of the *MYC* gene. In addition, we found that some cases of plasmablastic lymphoma have *STAT3* activation due to somatic mutations in the *STAT3*-SH2 domain which may increase MYC expression.

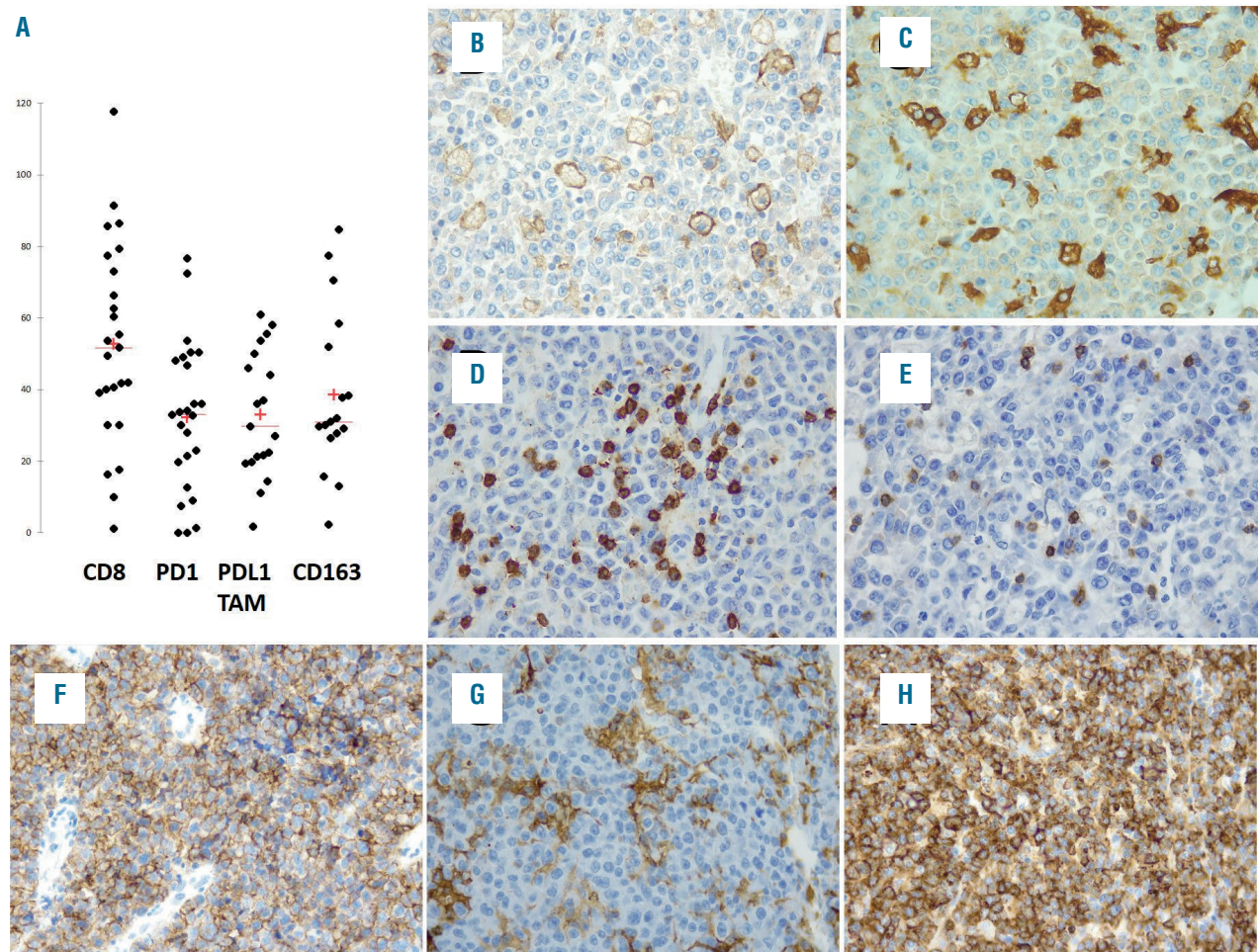


Figure 5. Phenotype of microenvironmental and neoplastic cells in plasmablastic lymphoma. (A) Scattergram illustrating the mean and range of expression values after quantification of the immunohistochemical expression of CD8, PD1 in lymphocytes and PD-L1 and CD163 in histiocyte/dendritic cell populations. (B) Representative image of a case with a mean of 36 PD-L1-positive non-neoplastic cells. (C) The same case showed a mean of 37 CD163-positive histiocytes. (D) The mean expression of CD8-positive cells in this representative case was 53. (E) PD1 identified a different T-cell subpopulation (mean of 36 PD1-positive cells in this representative example, case n. 25). (F) PD-L1 expression by neoplastic cells was identified in five out of 24 cases evaluated (20%). (G) MHCII protein/HLA (DP, DR) was, in most cases, restricted to histiocyte and endothelial cell populations. (H) MHCII protein/HLA (DP, DR) expression was identified in the neoplastic cells in three out of 25 cases tested (12%). Two of the three cases showed cytoplasmic granular and membranous staining (as illustrated in the figure) and one case had a membranous pattern.

notype, phospho-STAT3 expression has been found to be associated with the presence of ALK rearrangements and overexpression.²⁰ Importantly, STAT3 activation, due to somatic mutations in the *STAT3*-SH2 domain may contribute to *MYC* overexpression, as previously described in DLBCL.¹⁸ In addition, one case in our series showed concurrent *STAT3* SH2 mutations and phospho-STAT3 (Tyr705) expression and PD-L1 overexpression, confirming previous results in other lymphoma types suggesting that STAT3 activation triggers PD-L1 overexpression.²¹

STAT3 somatic mutations in PBL have not been previously described so far and may have therapeutic implications for the clinical testing of STAT3 inhibitors in these patients.

Interestingly the pattern of somatic mutations in EBV-negative disease was more heterogeneous. Mutations involving BCR activation, TLR/NFκB, histone modifying genes and the NOTCH pathway were found in eight cases (Table 1, Figure 1). *MYD88*pL265P mutation, involving the TIR domain of the *MYD88* gene, has been previously described in activated B-cell-type DLBCL, in primary central nervous system lymphoma and in other DLBCL in

immune privileged sites^{22,23} as well as in lymphoplasmacytic lymphoma/Waldenström macroglobulinemia²⁴ and leads to downstream activation of the IRAK4/IRAK1/TRAF6 complex and NFκB activation. The pattern of mutations in *CD79A/B* in PBL cases was distinct from that found in DLBCL NOS. Mutations in *CD79A/B* were found located outside the ITAM domains related with constitutive BCR activation in activated B-cell-type DLBCL.²⁵ NOTCH pathway genes that were mutated were *NOTCH2*, *NOTCH1* and *SGK1*. *NOTCH2*pR2400* is a nonsense mutation that truncates the PEST domain of the NOTCH2 protein and has already been described in B-cell non-Hodgkin lymphomas, including DLBCL NOS.²⁶ PEST domain-truncating mutations have been found in multiple tumor types and functional studies suggest that this class of mutations can be targeted with Notch inhibitors including γ secretase inhibitors.²⁷ *NOTCH1*pP401L was reported in chronic lymphocytic leukemia in a previous study²⁸ and lies within the calcium-binding EGF-like domains repeat. Mutations in *SGK1* involved the *SGK1*pS451F and *SGK1*pA380V point mutations and the *SGK1*pK136* truncating mutation. These

mutations have not been previously described in DLBCL NOS.²⁶ SGK1 has been suggested to be a negative regulator of NOTCH signaling, enhancing NOTCH protein degradation and reducing its activation by γ -secretase.²⁹ Other mutations found were *SMARCA4*pR1005Q and *TP53*pR273H.

Of note MAPK/ERK pathway-activating mutations involving *BRAF* (*BRAF*pV600E, *BRAF*pG469A) were found in two cases, both EBV-negative. *BRAF* mutations have been observed, rarely, in related neoplasms such as multiple myeloma. Previous studies found *BRAF* mutations in 4% of cases of multiple myeloma;³⁰ they were associated with aggressive clinical features, a plasmablastic phenotype and clonal evolution,^{31,32} with obvious clinical implications for targeted therapy.

In addition to the genetic profile of the cases, we also explored the composition of the tumor microenvironment and the expression of immune-checkpoint markers in both the neoplastic and other lymphoid and histiocytic/dendritic populations. Our results confirm those of previous studies showing an enrichment in TAM that express CD163 and PD-L1. The PBL also had a significant population of CD8-positive T cells, irrespective of the almost absent expression of MHCII/HLA by the neoplastic cells.⁹ Importantly, together with CD8-positive T cells, there was a distinct population of PD1-positive T cells. In the PBL cases that we studied, EBV did not influence the immune populations, with regards to the content of TAM and CD8-positive and PD1-positive T cells quantified in the tissue. Furthermore, in our series, PD-L1 expression by the neoplastic cells was found in 20% of the cases analyzed, similarly to previously published series,⁸ and there was no association between EBV infection by tumor cells and PD-L1 expression, since PD-L1 was found in both EBV-positive and EBV-negative variants and most of the EBV-positive cases were PD-L1-negative. These findings are in agreement with previously published data on PBL, with variable expression of PD-L1 ranging from 20 to 44%, by the neoplastic population.^{8,33} In our series, however, we did not confirm an association between EBV infection and PD-L1 expression, suggested by others.⁸ This difference may be due to a combination of factors, including different clones used for the detection of PD-L1 expression (22C3 clone in this study, SP142 in others⁹) and different quantification and statistical methods used. In addition another biological factor related to the uncommon PD-L1 expression in PBL cases could be related to the usual latency pattern found in these cases, since PD-L1 expression in EBV-positive post-transplant lymphoproliferative disorder has been strongly associated with EBV latency patterns 2 and 3³⁴

while PBL cases usually have EBV latency pattern 1.⁷ Notably one of our cases points to STAT3 activation as a potential cause for PD-L1 overexpression in PBL. Collectively our results on the microenvironment and immune-checkpoint expression in PBL indicate a potential for immune checkpoint interference in patients with this type of lymphoma.

In summary, in this study we found that the mutational profile of PBL was related to EBV infection in the tumor cells and identified recurrent genetic events in *MYC*, *STAT3* and *PRDM1*/Blimp1 that were associated with EBV-positive disease. *MYC* genetic alterations (including translocations and amplification) and SH2 domain *STAT3* mutations led to *MYC* and phospho-STAT3 (Tyr705) protein overexpression, respectively. Other somatic mutations including *BRAF*pV600E, *MYD88*pL265P, *NOTCH2*pR2400* and *TP53*pR273H, appeared in EBV-negative disease, suggesting an overlapping mutational profile with both multiple myeloma and DLBCL NOS. Furthermore, the tumor microenvironment in PBL was characterized by an enrichment in PD-L1-positive TAM and PD1 reactive T lymphocytes with expression of PD-L1 by the neoplastic tumor cells in a fraction of cases. Novel molecular targets derived from the present study include *MYC* and *STAT3* activation, MAPK/ERK and NOTCH2 pathway mutations and immune-checkpoint interference.

Disclosures

No conflicts of interest to disclose.

Contributions

JGR and NMM performed research, analyzed data and approved the paper. SGV, RT, SB and MG analyzed data and approved the paper. SL and EDA performed research, provided clinical data and approved the paper. AGM and AGP performed research and approved the paper. CV and JK provided clinical data and approved the paper. SMM designed and performed research, analyzed data, and wrote and approved the paper.

Funding

This study was supported by grants from MINECO (PI16/1397, SMM, Principal Investigator) and IDIVAL (NEXTVAL 15/09, SMM, Principal Investigator). NMM was supported by Asociación Española contra el Cáncer (AECC).

Acknowledgments

The authors acknowledge the Valdecilla Tumor Biobank Unit (Tissue Node, PT13/0010/0024) for their skillful handling and processing of tissue samples and all their clinical colleagues and pathologists who provided clinical data and samples for this research study.

References

1. Swerdlow S, Campo E, Harris NL, et al. (Editors). WHO Classification of Tumours of Haematopoietic and Lymphoid Tissues. Fourth edition. IARC 2008.
2. Campo E, Swerdlow SH, Harris NL, Pileri S, Stein H, Jaffe ES. The 2008 WHO classification of lymphoid neoplasms and beyond: evolving concepts and practical applications. *Blood*. 2011;117(19):5019-5032.
3. Delecluse HJ, Anagnostopoulos I, Dallenbach F, et al. Plasmablastic lymphomas of the oral cavity: a new entity associated with the human immunodeficiency virus infection. *Blood*. 1997;89(4):1413-1420.
4. Montes-Moreno S, Gonzalez-Medina AR, Rodriguez-Pinilla SM, et al. Aggressive large B-cell lymphoma with plasma cell differentiation: immunohistochemical characterization of plasmablastic lymphoma and diffuse large B-cell lymphoma with partial plasmablastic phenotype. *Haematologica*. 2010;95(8):1342-1349.
5. Colomo L, Loong F, Rives S, et al. Diffuse large B-cell lymphomas with plasmablastic differentiation represent a heterogeneous group of disease entities. *Am J Surg Pathol*. 2004;28(6):736-747.
6. Chapman J, Gentles AJ, Sujoy V, et al. Gene expression analysis of plasmablastic lymphoma identifies downregulation of B-cell receptor signaling and additional unique transcriptional programs. *Leukemia*. 2015;29(11):2270-2273.
7. Gravelle P, Péricart S, Tosolini M, et al. EBV infection determines the immune hall-

- marks of plasmablastic lymphoma. *Oncoimmunology*. 2018;7(10):e1486950.
8. Laurent C, Fabiani B, Do C, et al. Immune-checkpoint expression in Epstein-Barr virus positive and negative plasmablastic lymphoma: a clinical and pathological study in 82 patients. *Haematologica*. 2016;101(8):976-984.
 9. Schmelz M, Montes-Moreno S, Piris M, Wilkinson ST, Rimsza LM. Lack and/or aberrant localization of major histocompatibility class II (MHCII) protein in plasmablastic lymphoma. *Haematologica*. 2012;97(10):1614-1616.
 10. Valera A, Balagué O, Colomo L, et al. IG/MYC rearrangements are the main cytogenetic alteration in plasmablastic lymphomas. *Am J Surg Pathol*. 2010;34(11):1686-1694.
 11. Tadesse-Heath L, Meloni-Ehrig A, Scheerle J, Kelly JC, Jaffe ES. Plasmablastic lymphoma with MYC translocation: evidence for a common pathway in the generation of plasmablastic features. *Mod Pathol*. 2010;23(7):991-999.
 12. Montes-Moreno S, Martinez-Magunacelaya N, Zecchini-Barrese T, et al. Plasmablastic lymphoma phenotype is determined by genetic alterations in MYC and PRDM1. *Mod Pathol*. 2017;30(1):85-94.
 13. Munevver C, Rong HR, Chineke I, et al. Genetic analysis of plasmablastic lymphomas in HIV (+) patients reveals novel driver regulators of the noncanonical NF- κ B pathway. *Blood*. 2018;132(Suppl 1):1565.
 14. Swerdlow SH, Campo E, Harris NL, et al. (Editors). WHO Classification of Tumours of Haematopoietic and Lymphoid Tissues. Revised fourth edition. IARC. Lyon 2017.
 15. Montes-Moreno S, Martinez-Magunacelaya N, Zecchini-Barrese T, et al. Plasmablastic lymphoma phenotype is determined by genetic alterations in MYC and PRDM1. *Mod Pathol*. 2017;30(1):85-94.
 16. Pasqualucci L, Neumeister P, Goossens T, et al. Hypermutation of multiple proto-oncogenes in B-cell diffuse large-cell lymphomas. *Nature*. 2001;412(6844):341-346.
 17. Loghavi S, Alayed K, Aladily TN, et al. Stage, age, and EBV status impact outcomes of plasmablastic lymphoma patients: a clinicopathologic analysis of 61 patients. *J Hematol Oncol*. 2015;8:65.
 18. Sarosiek KA, Malumbres R, Nechushtan H, Gentles AJ, Avisar E, Lossos IS. Novel IL-21 signaling pathway up-regulates c-Myc and induces apoptosis of diffuse large B-cell lymphomas. *Blood*. 2010;115(3):570-580.
 19. Ohgami RS, Ma L, Monabati A, Zehnder JL, Arber DA. STAT3 mutations are present in aggressive B-cell lymphomas including a subset of diffuse large B-cell lymphomas with CD30 expression. *Haematologica*. 2014;99(7):e105-107.
 20. Valera A, Colomo L, Martinez A, et al. ALK-positive large B-cell lymphomas express a terminal B-cell differentiation program and activated STAT3 but lack MYC rearrangements. *Mod Pathol*. 2013;26(10):1329-1337.
 21. Tabanelli V, Corsini C, Fiori S, et al. Recurrent PDL1 expression and PDL1 (CD274) copy number alterations in breast implant-associated anaplastic large cell lymphomas. *Hum Pathol*. 2019;90:60-69.
 22. Ngo VN, Young RM, Schmitz R, et al. Oncogenically active MYD88 mutations in human lymphoma. *Nature*. 2011;470(7332):115-119.
 23. Chapuy B, Roemer MG, Stewart C, et al. Targetable genetic features of primary testicular and primary central nervous system lymphomas. *Blood*. 2016;127(7):869-881.
 24. Treon SP, Xu L, Yang G, et al. MYD88 L265P somatic mutation in Waldenstrom's macroglobulinemia. *N Engl J Med*. 2012;367(9):826-833.
 25. Davis RE, Ngo VN, Lenz G, et al. Chronic active B-cell-receptor signalling in diffuse large B-cell lymphoma. *Nature*. 2010;463(7277):88-92.
 26. Karube K, Enjuanes A, Dlouhy I, et al. Integrating genomic alterations in diffuse large B-cell lymphoma identifies new relevant pathways and potential therapeutic targets. *Leukemia*. 2018;32(3):675-684.
 27. Wang K, Zhang Q, Li D, et al. PEST domain mutations in Notch receptors comprise an oncogenic driver segment in triple-negative breast cancer sensitive to a γ -secretase inhibitor. *Clin Cancer Res*. 2015;21(6):1487-1496.
 28. Sutton LA, Ljungström V, Mansouri L, et al. Targeted next-generation sequencing in chronic lymphocytic leukemia: a high-throughput yet tailored approach will facilitate implementation in a clinical setting. *Haematologica*. 2015;100(3):370-376.
 29. Mo JS, Ann EJ, Yoon JH, et al. Serum- and glucocorticoid-inducible kinase 1 (SGK1) controls Notch1 signaling by downregulation of protein stability through Fbw7 ubiquitin ligase. *J Cell Sci*. 2011;124(Pt 1):100-112.
 30. Chapman MA, Lawrence MS, Keats JJ, et al. Initial genome sequencing and analysis of multiple myeloma. *Nature*. 2011;471(7339):467-472.
 31. Bohn OL, Hsu K, Hyman DM, Pignataro DS, Giralt S, Teruya-Feldstein J. BRAF V600E mutation and clonal evolution in a patient with relapsed refractory myeloma with plasmablastic differentiation. *Clin Lymphoma Myeloma Leuk*. 2014;14(2):e65-68.
 32. Andriulis M, Lehnert N, Capper D, et al. Targeting the BRAF V600E mutation in multiple myeloma. *Cancer Discov*. 2013;3(8):862-869.
 33. Chen BJ, Chapuy B, Ouyang J, et al. PD-L1 expression is characteristic of a subset of aggressive B-cell lymphomas and virus-associated malignancies. *Clin Cancer Res*. 2013;19(13):3462-3473.
 34. Vellozo L, Teixeira C, Castrejón N, et al. Clinicopathological evaluation of the programmed cell death 1 (PD1)/programmed cell death-ligand 1 (PD-L1) axis in post-transplant lymphoproliferative disorders: association with Epstein-Barr virus, PD-L1 copy number alterations, and outcome. *Histopathology*. 2019;75(6):799-812.